Monitoring Regional Evapotranspiration Using SEBAL Approach and MODIS Time-Series Data in the Center of Rice Producing Regions in West Java – Indonesia

Dewi Kania Sari [1,2]
Ishak H. Ismullah [1], **Widyo Nugroho Sulasdi** [1], **Agung Budi Harto** [1]

[1] Geodetic & Geomatics Engineering Study Program - Institut Teknologi Bandung (ITB), Indonesia
[2] Geodetic Engineering Study Program - Institut Teknologi Nasional (Itenas) Bandung, Indonesia

E-mail: dewiks@yahoo.com

ABSTRACT

Irrigated agriculture is one of the biggest consumers of fresh water. Considering the growing water scarcity, it is essential to use irrigation water more efficiently. Evapotranspiration from irrigated land is a useful indicator to evaluate the adequacy and reliability of irrigation as well as the equity in water use. Conventional methods to compute evapotranspiration are based on climate data and only provide point estimates. Better regional estimation of evapotranspiration can be retrieved from satellite remote sensing. Such methods provide a powerful means to compute actual evapotranspiration (ET_a) from individual pixel to an entire image. One of the most popular remote sensing algorithms in the retrieval of ET_a is SEBAL (Surface Energy Balance Algorithm on Land). In SEBAL, ET_a is evaluated as the residual when net radiation, soil heat flux, and sensible heat flux are retrieved with satellite data combined with some surface observations. SEBAL has been used operationally in many countries since 1990's, but its application in Indonesia was very limited. This study aims to evaluate spatio-temporal variation of ET_a of paddy field in the northern West Java as one of the most important rice-producing regoins in Indonesia. We used SEBAL approach to monitor ET_a in the region. Time-series MODIS (MOderate resolution Imaging Spectroradiometer) data of May-August 2004 have been used to evaluate daily and seasonal ET_a over paddy field in study area. This paper presents the findings of the study.

Key words: evapotranspiration, SEBAL, MODIS, paddy field, West Java

1. INTRODUCTION

In the future, less water will be available for agricultural production due to competition with the industrial and domestic sectors, while at the same time food production must be increased to feed the growing population (Zwart & Bastiaanssen 2007). Irrigated agriculture is one of the biggest consumers of fresh water. Considering the growing water scarcity, it is essential to use irrigation water more efficiently. Evapotranspiration (*ET*) from irrigated land is a useful indicator to evaluate the adequacy and reliability of irrigation as well as the equity in water use. Over most of the global land area, evapotranspiration (*ET*) is the second largest (after precipitation) component of the water cycle. It is a product of complex interactions among atmospheric demand, and soil and vegetation conditions which control supply. In general, evapotranspiration is poorly observed as compared with the other major terms in the surface water balance.

Conventional methods to compute evapotranspiration are based on climate data (Allen *et al.* 1998). In these methods routinely collected climatic data are used to compute evapotranspiration (*ET*) for a reference crop and then using an area-specific crop coefficient (K_c), crop water requirement or evapotranspiration is calculated for different growth stages of the crop under investigation. Cropped area and K_c are not known with certainty and general values from the literature are usually used to estimate *ET*. Such estimates may differ considerably from the actual evapotranspiration (ET_a), due to variations in planting dates, crop growth stages and root-zone moisture conditions. For these reasons, it is difficult using traditional methods to estimate space-time variations in crop water use based on point observations of meteorological quantities (Ahmad *et al*. 2006). Moreover, conventional techniques provide point estimates and often it is not practically possible to capture all the spatial variation at broad scales such as river basins, which are increasingly recognized as the management unit for irrigation and other water uses.

Better regional estimation of evapotranspiration can be retrieved from satellite remote sensing. Such methods provide a powerful means to compute actual evapotranspiration (ET_a) from individual pixel to an entire image. One of the most popular remote sensing algorithms in the retrieval of ET_a is Surface Energy Balance Algorithm on Land (SEBAL). SEBAL is a robust remote sensing model that can be applied to estimate the different components of the energy balance of the earth surface and thus also actual evapotranspiration (ET_a) (Bastiaanssen *et al*., 1998a; 1998b; 2005). In SEBAL, ET_a is evaluated as the residual when net radiation, soil heat flux, and sensible heat flux are retrieved with satellite data combined with some surface observations. As surface energy balances and crop water stress are directly linked to agricultural water use, ET_a variations in space and time are thought to be highly indicative for the adequacy and reliability of irrigation as well as the equity in water use. SEBAL has been used operationally in many countries since 1990's, but its application in Indonesia was very limited.

This study aims to evaluate spatio-temporal variation of ET_a of paddy field in the northern West Java as one of the most important rice-producing regoins in Indonesia. In this study, SEBAL was applied to estimate daily and seasonal ET_a over paddy field in the study area using time-series MODIS (MOderate resolution Imaging Spectroradiometer) data of May – August 2004.

2. STUDY AREA

The study area located in the northern West-Java Province which comprises 9 districts (Figure 1). This area has about 6681 km^2 of paddy field and roles as the center of rice producing regions in West-Java. BPS-Statistics Indonesia reported that the province of West Java is the prime contributor of the national rice production with 17.10% market share average (2006-2008). The province of West Java has the widest area of paddy field with market share of 15.10% to the national paddy field area. The climate of the area is humid trophic with annual average precipitation about 1500 to 2000 mm. The common annual rice cropping cycles on Java Island consists of three periods: wet season (WS) (October/November to January/February), dry season I (DS I) (February/March to May/June), and dry season II (DS II) (June/July to September/October).

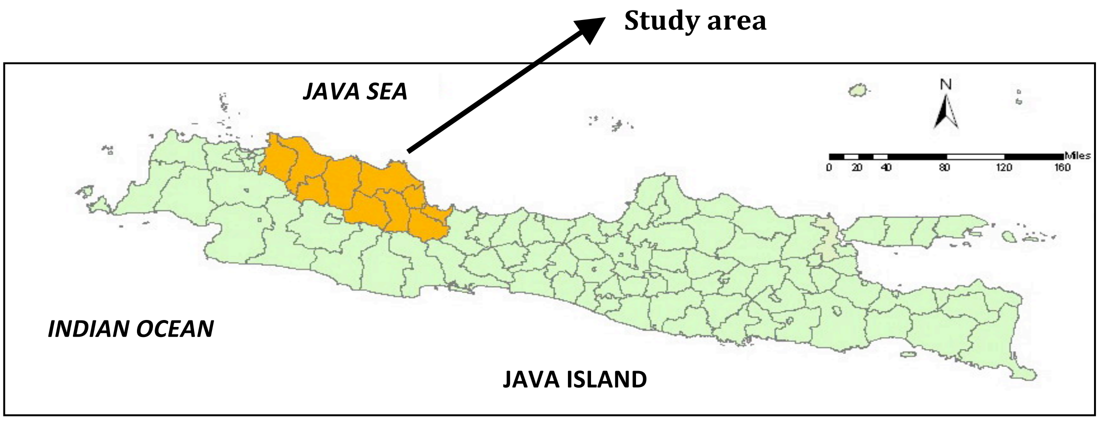

Figure 1. Location of study area in the Northern West-Java Province

3. MATERIALS & METHODS

3.1 Data

In this study we employed time-series MODIS data of level 2 (L2) and 3 (L3) (see details in Table 1. MODIS is the key instrument aboard the Terra (EOS AM-1) satellite. Terra MODIS is viewing the entire Earth's surface every 1 to 2 days, acquiring data in 36 spectral bands, or groups of wavelengths. MODIS sensor on Terra platform has a spectral resolution featuring 36 bands ranging from 250 to 1000 meters spatial resolution. Acquisition of L2 and L3 MODIS image was done through the NASA website using ftppull protocol.

Table 1. MODIS data used in this study

MODIS Data	Description	Spatial Resolution	Image Acquisition Dates
MOD09GA	Surface reflectance band 1-7, daily	1000 m	11 May, 2004 2, 16, 30 June, 2004 23, 30 July, 2004 12, 19, 29 August, 2004
MOD11A1	Land Surface Temperature & Emissivity, daily	1000 m	
MOD09A1	Surface reflectance band 1-3, 8 day	500 m	8 May, 2004 1, 17 June, 2004 3, 19, 27 July, 2004 12, 20, 28 August, 2004

The preprocessing parameters required for SEBAL include the Normalized Difference Vegetation Index (NDVI), surface emissivity, broadband surface albedo, and land surface temperature (LST). Broadband surface albedo was derived from MOD09GA data. The LST and emissivity were directly taken from MOD11A1 data. We calculated NDVI and EVI (Enhanced Vegetation Index) from MOD09A1 data.

In addition to satellite data, SEBAL approach needs some weather data (temperature, wind speed, relative humidity, and solar radiation). For this study, we obtained weather data from 9 weather stations distributed over northern West Java. Inverse Distance Weighting (IDW) technique was used to interpolate the data. DEM (Digital Elevation Model) of the study area required for SEBAL application was derived from SRTM data. The data was downloaded from website of the International Centre for Tropical Agriculture (CIAT).

3.2 SEBAL Approach

The SEBAL procedures consists of a suite of equations that solve the complete energy balance,

$$\lambda E = R_n - G - H \tag{1}$$

where λE = latent heat flux (the energy used to evaporate water); R_n = net radiation at the surface; G = soil heat flux; and H = sensible heat flux to the air. R_n is computed from satellite-measured broadband surface albedo, vegetation index and surface temperature, along with ground measurements of global radiation. G is predicted using vegetation indices computed from spectral data and net radiation. H is estimated from surface temperature, surface roughness, and wind speed. All computations are made specific to each pixel in the image. A number of publications have been released on SEBAL approach and its' applications describing the entire procedure (Bastiaanssen *et al*. 1998a; Tasumi *et al.* 2000; Bastiaanssen *et al*. 2005).

Net radiation R_n is calculated by surface radiation balance:

$$R_n = (1 - \alpha_o)R_{s\downarrow} + R_{L\downarrow} - R_{L\uparrow} + (1 - \varepsilon_o)R_{L\downarrow} \tag{2}$$

where $Rs_{\downarrow}$ is incoming short radiation, $R_{L\downarrow}$ is incoming long wave radiation, and $R_{L\uparrow}$ is outgoing long wave radiation, α_o and ε_o are surface albedo and emissivity respectively; all are calculated by standard algorithms and/or land surface parameterization schemes.

Soil heat flux G is evaluated by an empirical relation with net radiation and a few other surface parameters, such as applied by Tasumi *et al*. (2000):

$$G = 0.30(1 - 0.98NDVI^4)R_n \tag{3}$$

Sensible heat flux H is calculated by using the temperature difference between air and surface temperatures, and surface aerodynamic resistance to heat flow:

$$H = \rho C_p \frac{T_s - T_a}{r_a} \tag{4}$$

where T_s is surface temperature retrieved by remote sensing, T_a is air temperature at specific height. ρ and C_p are air density and air specific heat at constant pressure respectively. r_a is the surface aerodynamic resistance to heat transfer, calculated by:

$$r_a = \frac{ln\left(\frac{z}{z_o}\right) - \psi_h\left(\frac{z}{L}\right) + \psi_h\left(\frac{z_o}{L}\right)}{ku_*} \tag{5}$$

where ψ_h is the Monin-Obukhov stability function. L is Obukhov length. z_o is surface roughness length. The innovative point of SEBAL is the utilization of two reference pixels, 'hot' and 'cold', in the image to fix boundary conditions for the air-surface temperature difference, and assumes a linear function between this difference and the radiometric surface temperature. An iterative way started from neutral stability assumptions is used in the calculation of friction velocity (u_*), r_a, and then the surface sensible heat flux H.

The latent heat flux, λE, is the residual term of the energy balance, and is used to compute the instantaneous evaporative fraction, Λ:

$$\Lambda = \frac{\lambda E}{\lambda E + H} = \frac{\lambda E}{R_n - G} \tag{6}$$

The instantaneous evaporative fraction, Λ, expresses the ratio of the actual to crop evaporative demand when the atmospheric moisture conditions are in equilibrium with the soil moisture conditions. The evaporative fraction tends to be constant during daytime hours. The difference between the instantaneous evaporative fraction at the moment of satellite overpass, and the evaporative fraction derived from the 24-hour integrated energy balance is marginal, and may be neglected (Farah 2001; Ahmad *et al*. 2006). For time scales of 1 day or longer, G can be ignored and net available energy ($R_n - G$) reduces to net radiation (R_n). For daily time scale, ET_{a24} (mm d^{-1}) can be computed as:

$$ET_{a24} = \frac{86400 \times 10^3}{\lambda \rho_w} \Lambda R_{n24} \quad (7)$$

where R_{n24} is the 24-hour average net radiation, λ (J kg^{-1}) is the latent heat of vaporization and ρ_w (kg m^{-3}) is the density of water. The equation for calculating R_{n24} under conditions of clear sky (all day) is (Tasumi *et al*. 2000):

$$R_{n24} = (1 - \alpha_o) R_{a24} \tau_{sw} - 110 \tau_{sw} \quad (8)$$

where R_{a24} is daily extraterrestrial radiation, α_o is surface albedo, and τ_{sw} is one-way transmittance. The accumulated evapotranspiration can be predicted from the time integrated equation:

$$ET_{adt} = \frac{86400 \times 10^3}{\lambda \rho_w} \Lambda R_{n24,dt} \quad (9)$$

where ET_{adt} (mm $interval^{-1}$) is the actual evapotranspiration during interval d*t* measured in days and $R_{n24,dt}$ (W m^{-2}) is the average R_{n24} value for the time interval *dt*. The evaporative fraction, Λ, is assumed to be constant during interval d*t*. Farah (2001) found that the accumulated evapotranspiration for a period of 10 to 20 days can be predicted satisfactorily from Eq.(9). The seasonal actual evapotranspiration (ET_{as}) is obtained by totaling the values of ET_{adt} from the beginning to the end of the season:

$$ET_{as} = \sum_{i=1}^{n} ET_{adti} \quad (10)$$

where ET_{ai} is the accumulated actual evapotraspiration for interval dt_i, n is the sum of accumulated ET_a calculated during the season. In this study the seasonal ET_a was calculated for the cropping season, from May 1 to August 31, 2004.

4. RESULTS & DISCUSSIONS

Figure 2 shows the maps of daily actual evapotranspiration using MODIS data for the study area on May 11, June 2, 16, and 30, July 23 and 30, August 12, 19, and 29, 2004. Daily actual evapotranspiration (ET_{a24}) maps clearly indicate spatio-temporal variation of ET_{a24} across paddy field in the study area. The estimated daily evapotranspiration ranged from 0 to 6.7 mm/day and the average values of ET_{a24} for the whole area ranged from 1.1 to 3.0 mm/day. Table 2 shows the statistics of 9 daily actual evapotranspirations that were analysed.

Even with 1 km spatial resolution (Fig. 2), dryer areas (orange color) can be differentiated from wet areas (green-blue colors). Higher values of ET_{a24} appear in the northern part of the study area, along the North Coast of West Java. Meanwhile, the southern parts show lower ET_{a24}. From May to June 2004, ET_{a24} mean values ranged from 2.5 to 2.9 mm/day, indicating no water stress in most of paddy field areas. Indication of water stress or agricultural drought occurred on July, 2004 with ET_{a24} mean values ranged from 1.2 to 1.5 mm/day. This result matched with the information reported by the Agricultural Deparment and a study conducted by Parwati (2008). On the middle of August 2004, the ET_{a24} values increased to 2.3 – 3.0 mm/day, but at the end of the month it decreased to only 1.1 mm/day. August 2004 was reported as the peak of dry season of the year.

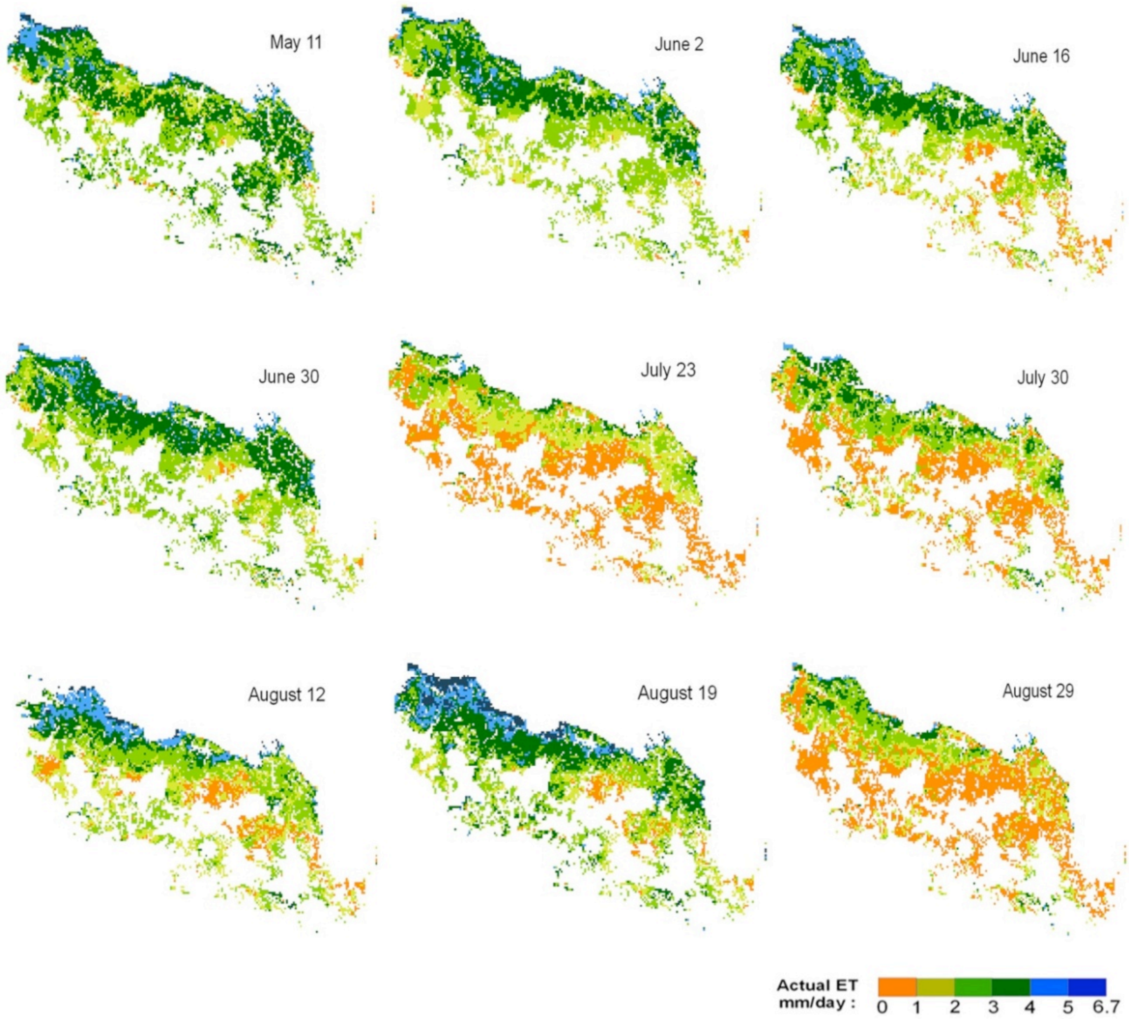

Figure 2. Spatio-temporal variation of daily actual evapotranspiration of paddy field area in the northern West Java retrieved from MODIS data

Table 2. Statistics of daily actual evapotranspiration of paddy field in northern West Java retrieved from MODIS data

Date	DOY	ET_{a24} Range (mm day^{-1})	ET_{a24} Mean (mm day^{-1})	St. Dev (mm day^{-1})
May 11, 2004	132	0 – 6.1	2.9	0.8
June 2, 2004	154	0 – 5.6	2.7	0.8
June 16, 2004	168	0 – 6.0	2.5	1.1

June 30, 2004	182	0 – 5.3	2.8	0.8
July 23, 2004	205	0 – 4.5	1.2	1.1
July 30, 2004	212	0 – 6.1	1.5	1.2
August 12, 2004	225	0 – 6.7	2.3	1.2
August 19, 2004	232	0 – 5.1	3.0	1.2
August 29, 2004	242	0 – 5.2	1.1	1.2

Seasonal actual evapotranspiration (ET_{as}) was calculated for the cropping season from May 1 to August 31, 2004. Figure 3 shows spatial variation of the seasonal actual ET accross the study area. The estimated ET_{as} ranged from 54 to 679 mm/season with the mean value of 321 mm/season (Table 3). Generally, higher values of ET_{as} appear in northern area (shown in dark green dan blue colors) while lower values appear in southern area (in light green and orange colors). Highest ET_{as} occurred in northern part of Bekasi, Karawang, Subang, Indramayu, and Cirebon districts. Lowest ET_{as} (orange color) covered 2.3% of the paddy field area, spreaded in southern areas. The distributin of ET_{as} values presented in Table 4.

Since crop water requirement or evapotranspiration is different for any growing stages, the interpretation of the ET_a values depends critically on understanding vegetation phenology and cropping cycle at the time of image acquisiton. Low value of ET_a does not always designate the occurrence of crop water stress. Both crop growth stage and water stress might cause the low ET_a. We need further studies to interprete and evaluate ET_a values resulted from this study.

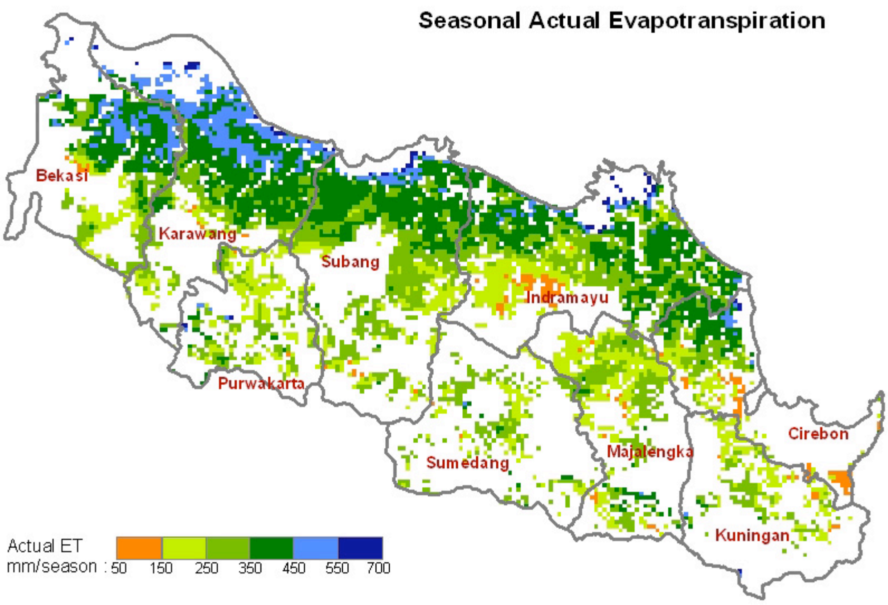

Figure 3. Seasonal actual evapotranspiration of paddy field area in northern West Java retrieved from MODIS data

Table 3. Statistics of seasonal actual evapotranspiration of paddy field in northern West Java

Area	6681 km^2
Mean ET_{as}	321 mm/season
Min. ET_{as}	54 mm/season
Max. ET_{as}	679 mm/season
ET_{as} stand. deviation	96 mm/season
ET_{as} coef. variation	0.3

Table 4. The distribution of seasonal actual evapotranspiration of paddy field in northern West Java

ET_{aseas} (mm/season)	Area (km^2)	% Area
50 – 150	155	2.3
150 – 250	1347	20.2
250 – 350	2145	32.1
350 – 450	1886	28.2
450 – 550	486	7.3
550 – 700	65	1.0
No Data (cloud)	597	9.0

5. CONCLUSIONS

The purpose of this study was to demonstrate the utilization of the SEBAL approach to monitor spatio-temporal variation of actual evapotranspiration for paddy field area in northern West Java. In this study 9 images of MODIS were used to solve net radiation, soil heat flux, and sensible heat flux components of the energy balance. Latent heat flux, the residual term of surface energy balance was used to compute actual evapotranspiration for every 1 km x 1 km pixel. The study results show that the average of daily actual evapotranspiration ranged from 1.1 to 2.9 mm/day, while seasonal actual evapotranspiration calculated from May 1 to August 31, 2004 ranged from 54 to 679 mm/season, with average value of 321 mm/season. The lowest evapotranspiration rates occurred in the end of July and August, 2004. The critical to the interpretation of the SEBAL results in paddy field area is knowledge of rice phenology and cropping calendars.

REFERENCES

Ahmad, M.-ud.-D., Biggs, T., Turral, H., Scott, C.A., 2006. Application of SEBAL approach and MODIS time-series to map vegetation water use patterns in the data scarce Krishna river basin of India. *Water Science & Technology* Vol.53, No. 10, 83-90.

Allen, R. G., L. S. Pereira, D. Raes, and M. Smith, 1998. *Crop evapotranspiration, guidelines for computing crop water requirements,* FAO Irrig. and Drain. Pap. 56, 300 pp., Food and Agric. Organ. of the U. N. (FAO), Rome, Italy.

Bastiaanssen, W.G.M., Noordman, E.J.M., Pelgrum, H., Davids, G., Allen, R.G., 2005. SEBAL for spatially distributed ET under actual management and growing conditions. *J. Irr. Drain. Eng*. 131, 85–93.

Bastiaanssen, W.G.M, Menenti, M., Feddes, R.A., Holtslag, A.A.M. 1998a. The Surface Energy Balance Algorithm for Land (SEBAL): Part 1 formulation. *Journal of Hydrology*. 212-213: 198-212.

Bastiaanssen, W.G.M., Pelgrum, H., Wang, J., Ma, Y., Moreno, J., Roerink, G.J., Van Der Wal, T., 1998b. The Surface Energy Balance Algorithm for Land (SEBAL): Part 2 validation. *Journal of Hydrology*. 212-213: 213-229.

Farah, H.O., 2001. Estimation of regional evaporation using detailed agrohidrological model. *J. of Hydr*. 229(1-2): 50-58.

Parwati, 2008. The agricultural drought monitoring in Indramayu District – West Java using remote-sensing-based indices. Presented at ASTW 8th, Manila, July 3rd 2008.

Tasumi, M., Bastiaanssen, W.G.M., Allen, R.G., 2000. Application of the SEBAL methodology for estimating consumptive use of water and stream flow depletion in the River Basin of Idaho through Remote Sensing. Appendix C: A step-by-step guide to running SEBAL. EOSDIS Project Final Report, The Raytheon Systems Company and the University of Idaho.

Zwart, S.J. and Bastiaanssen, W.G.M., 2007. SEBAL for detecting spatial variation of water productivity and scope for improvement in eight irrigated wheat systems. *Agric. Water Manage*. 89, 287-296.